

# CHAPTER 7

## Monotectic Alloy Systems

ANOTHER THREE-PHASE reaction of the eutectic class is the monotectic, in which one liquid phase decomposes with decreasing temperature into a solid phase and a new liquid phase:



Over a certain composition range, the two liquids are mutually immiscible, such as oil and water, and so constitute individual phases. The phase diagram shown in Fig. 7.1 gives the terminology for this type of system: monotectic point, monotectic reaction isotherm, hypomonotectic, and hypermonotectic. The phase diagram shows a dome-shaped region within which the two liquids mix and coexist. The maximum temperature of this dome,  $T_c$ , is called the critical (or consolute) temperature. It should be noted that the liquidus and solidus curves are differently located and that these have been designated as “upper” and “lower” to distinguish them. There is no special name for the boundary of the  $L_1 + L_2$  field; it is simply called the limit of liquid immiscibility. The eutectic reaction, depicted by dashed lines in this example, is included merely to carry the diagram into the temperature range where all phases are solid.

Liquid copper and liquid lead are completely soluble in each other at high temperatures. However, as shown in the Fig. 7.2 phase diagram, alloys containing between 36 and 87 wt% Pb separate into two liquids on further cooling. The two liquids coexist in the miscibility gap, or dome, that is typical of all alloys that undergo a monotectic reaction. During solidification of a copper-lead alloy containing 20 wt% Pb, the copper-rich  $\alpha$  phase forms first. The liquid composition shifts toward the monotectic composition of 36 wt% Pb. Then, the liquid transforms to more solid  $\alpha$  and a second liquid containing 87 wt% Pb. The lever rule shows that only a very small amount of the second liquid is present. On further cooling, the

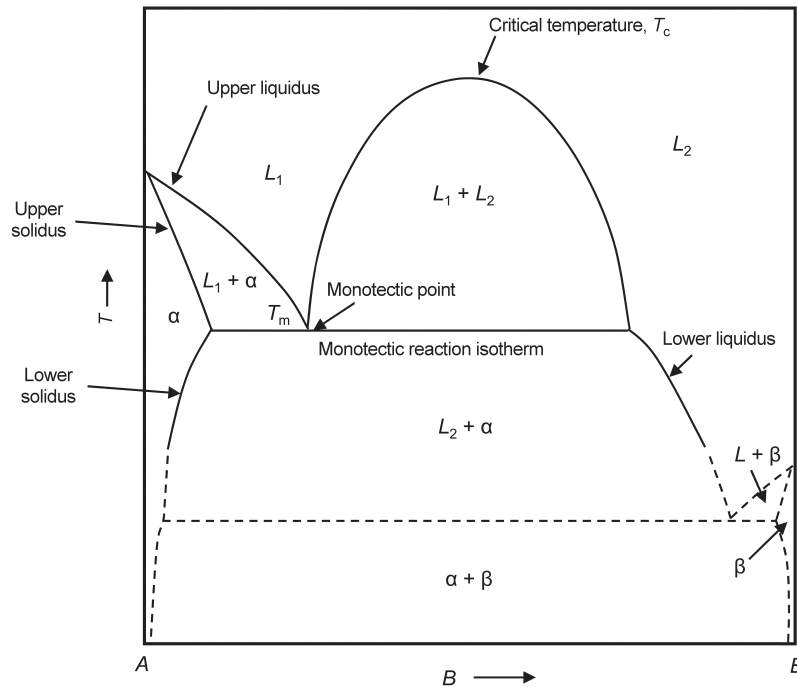


**Fig. 7.1** Monotectic phase diagram showing the invariant point,  $m$ , where liquid 1 ( $L_1$ ) transforms to another liquid ( $L_2$ ) and solid solution ( $\alpha$ ). Adapted from Ref 7.1

second liquid eventually undergoes a eutectic reaction, producing  $\alpha$  and  $\beta$ , where the  $\beta$  is almost pure lead. The microstructure of this alloy contains spherical  $\beta$  particles randomly distributed in a matrix of copper-rich  $\alpha$ .

Because of the continuity of the copper-rich phase in the monotectic structure, the physical properties of this alloy more nearly resemble those of copper than those of lead. Lead is often added to alloys because it makes the machining of the metal easier by reducing the ductility just enough to cause chips to break away, without seriously decreasing hardness and strength. Lead alloys are also used for bearings, where the continuous phase of the high-melting metal gives strength to the member, while the lead, occurring in pockets at the running surface, serves to reduce the friction between bearing and axle.

## 7.1 Solidification Structures of Monotectics

Monotectic alloys can be classified based on the difference between the critical temperature,  $T_c$ , and the monotectic temperature,  $T_m$ ; that is, the difference  $T_c - T_m$ . High-dome alloys have a large difference in  $T_c - T_m$

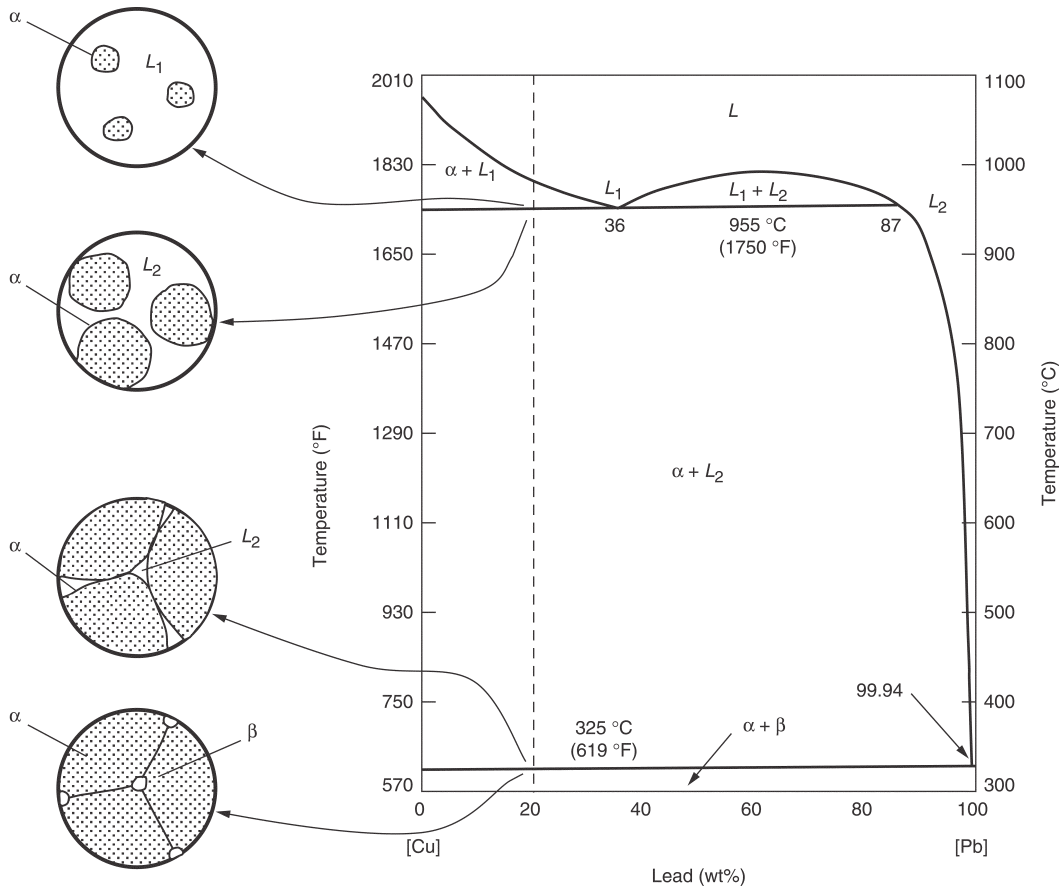


**Fig. 7.2** Monotectic reaction in copper-lead system. Source: Ref 7.2 as published in Ref 7.3

(hundreds of °C), while low-dome alloys have a small difference in  $T_c - T_m$  (tens of °C). They can also be classified based on the  $T_m/T_c$  ratio. High-dome alloys have  $T_m/T_c < 0.9$ , while low-dome alloys have  $T_m/T_c > 0.9$ .

The morphology of the microstructure produced during directional solidification is a function of the density difference between the two liquids, and of the wetting between  $L_2$  and  $\alpha$ . For low-dome alloys, the phases  $\alpha$  and  $L_2$  are separated by  $L_1$ , as shown in Fig. 7.3. At low growth rate,  $L_2$  particles are pushed by the solid-liquid interface (Fig. 7.3a). If the solidification velocity increases above a critical velocity ( $V_{cr}$ ),  $L_2$  is incorporated with formation of an irregular fibrous composite (Fig. 7.3b). Particle engulfment and pushing by solidifying interfaces has been observed experimentally.

Fibrous growth in the succinonitrile-20% ethanol system, in which the velocity is above the critical velocity for particle engulfment, is shown in Fig. 7.4. Similar microstructures are observed in metallic systems such as

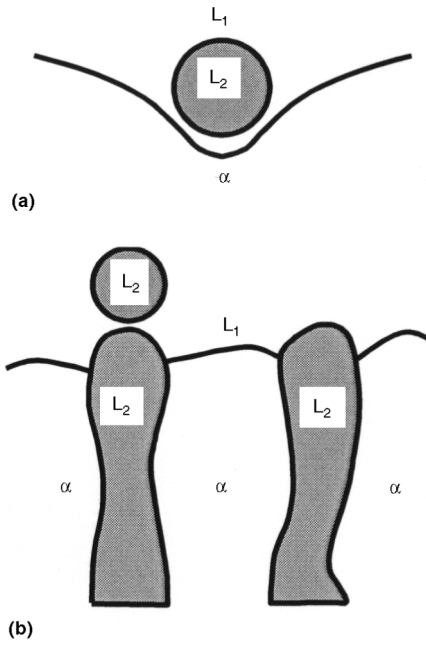


**Fig. 7.3** Monotectic solidification for low-dome alloys. (a) Low growth velocity. (b) High growth velocity. Source: Ref 7.4 as published in Ref 7.5

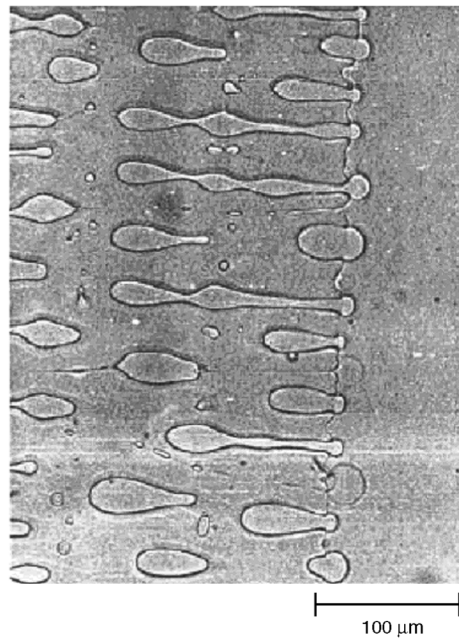


**Fig. 7.4** Growth front in succinonitrile-20 wt% ethanol, showing incorporation of ethanol droplets.  $V = 0.27 \mu\text{m/s}$ . Source: Ref 7.6 as published in Ref 7.5

Cu-60%Pb and Bi-50%Ga alloys, as shown in Fig. 7.5 for a copper-lead alloy. Note that the velocity in this microstructure is very high.

The range of existence of the fibrous composite is limited by the constitutional undercooling on one side and by the critical velocity of pushing-to-engulfment transition ( $V_{cr}$ ) on the other (Fig. 7.6). When the solidification velocity is smaller than  $V_{cr}$ , a banded structure may result. An example of such a structure is provided in Fig. 7.7. It is suggested that the  $L_2$  phase, which precipitates at the solid-liquid interface, piles up and covers the solid-liquid interface. This produces a lead-rich layer and increases the undercooling of the  $L_1$ - $L_2$  interface with respect to the

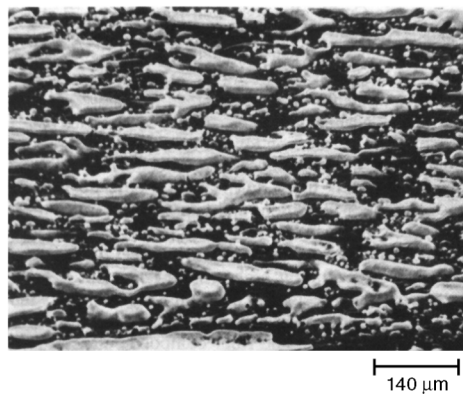


**Fig. 7.5** Microstructure of a Cu-70Pb alloy solidified at  $V = 778 \mu\text{m/s}$ . Solidification direction is right-to-left. Source: Ref 7.7 as published in Ref 7.5

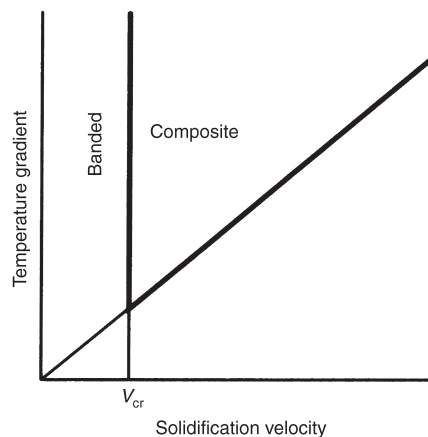


**Fig. 7.6** Restriction on composite growth imposed by the critical velocity for the pushing engulfment transition and by constitutional undercooling. Source: Ref 7.4 as published in Ref 7.5

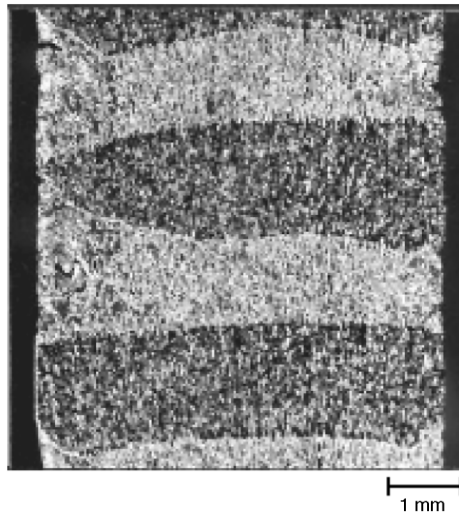


**Fig. 7.7** Microstructure of upward directional solidification of a Cu-37.7Pb alloy in longitudinal section.  $V = 4.4 \mu\text{m/s}$ . Source: Ref 7.8 as published in Ref 7.5

monotectic temperature. Then, nucleation of the  $\alpha$ -Cu phase occurs on the lead-rich layer. The temperature at the growth front is also returned to the monotectic temperature. The repetition of this process will result in the banded structure as shown in Fig. 7.8. It should be noted that some fibrous structure might form even in the case of banding (Fig. 7.9).

For high-dome alloys, the lowest energy exists when an  $\alpha$ - $L_2$  interface exists. Consequently,  $\alpha$  and  $L_2$  will grow together ( $L_2$  wets  $\alpha$ ), resulting in a regular (uniform) fibrous composite. The  $\lambda^2$ - $V$  relationship is approximately two orders of magnitude larger for irregular than for regular monotectic composites (with the exception of the aluminum-bismuth alloy) and approximately one order of magnitude higher for regular monotectic composites than for regular eutectics. The differences come from the controlling mechanism. For irregular fibrous eutectics, the controlling mechanism is the pushing-engulfment transition, which is a function of solidification velocity and surface energy. For regular fibrous monotectics, the spacing is controlled by surface energy. For eutectics, the spacing is controlled by diffusion.

#### ACKNOWLEDGMENT

Portions of this chapter came from “Fundamentals of Solidification,” by D.M. Stefanescu and R. Ruxanda in *Metallography and Microstructures*, Vol 9, *ASM Handbook*, ASM International, 2004.

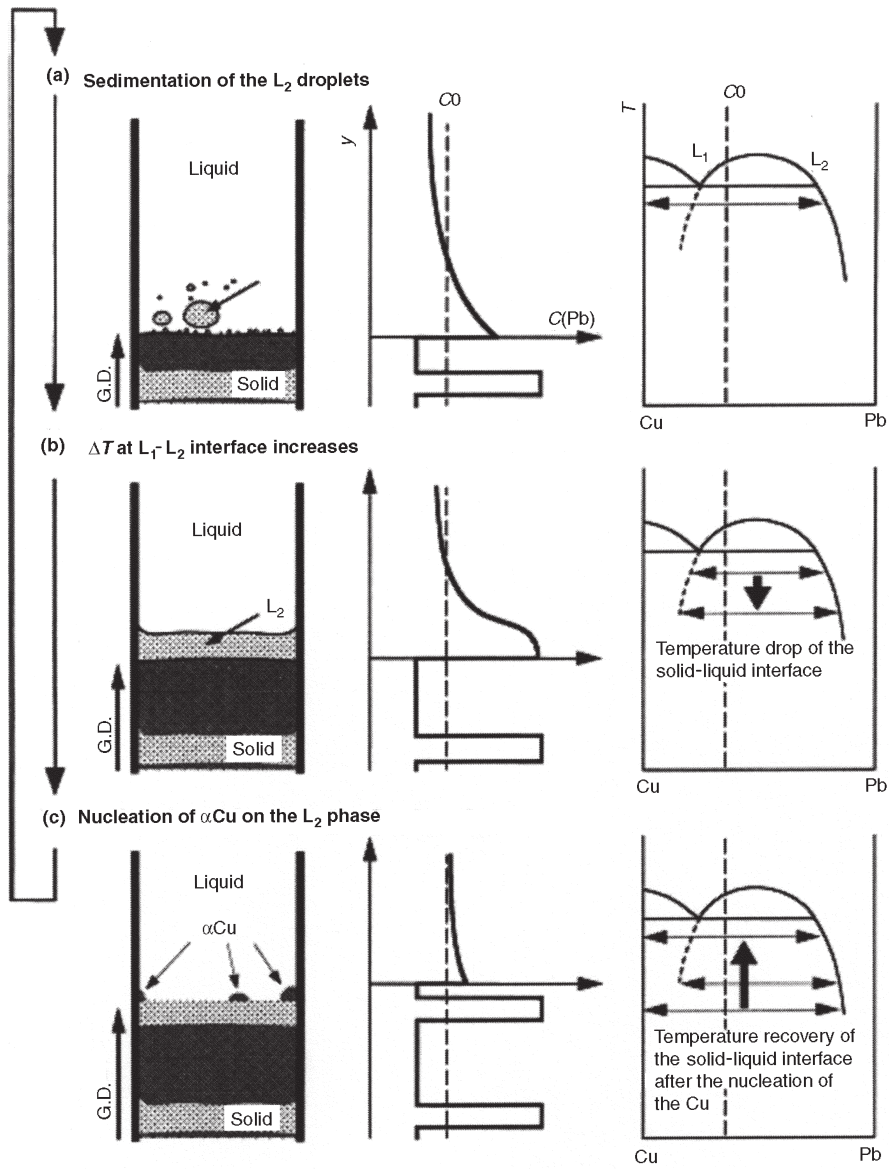


**Fig. 7.8** Forming mechanism of the banded structure of copper-lead alloy in upward directional solidification. G.D., growth direction. Source: Ref 7.8 as published in Ref 7.5

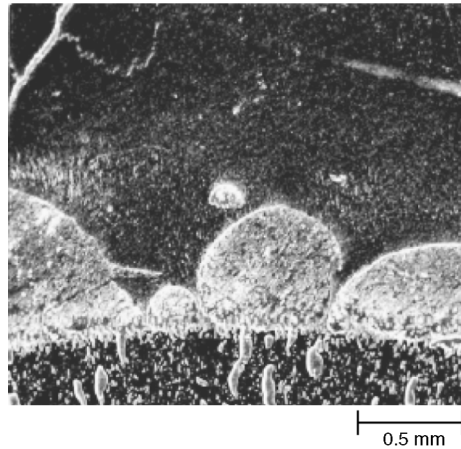


**Fig. 7.9** The solid-liquid interface covered with coalesced  $L_2$  phase. Cu-35.4Pb alloy, upward directional solidification,  $V = 2.2 \mu\text{m/s}$ . Source: Ref 7.8 as published in Ref 7.5

## REFERENCES

- 7.1 F.N. Rhines, *Phase Diagrams in Metallurgy*, McGraw-Hill, 1956, p 72
- 7.2 D.R. Askeland, *The Science and Engineering of Materials*, 2nd ed., PWS-KENT Publishing Co., 1989
- 7.3 F.C. Campbell, *Elements of Metallurgy and Engineering Alloys*, ASM International, 2008
- 7.4 D.M. Stefanescu, *Science and Engineering of Casting Solidification*, Kluwer Academic, 2002
- 7.5 D.M. Stefanescu and R. Ruxanda, Fundamentals of Solidification, *Metallography and Microstructures*, Vol 9, *ASM Handbook*, ASM International, 2004, p 71–92
- 7.6 R.N. Grugel, T.A. Lagrasso, and A. Hellawell, *Metall. Trans. A*, Vol 15A, 1984, p 1003–1010
- 7.7 B.K. Dhindaw, D.M. Stefanescu, A.K. Singh, and P.A. Curreri, *Metall. Trans. A*, Vol 19A, 1988, p 2839
- 7.8 I. Aoi, M. Ishino, M. Yoshida, H. Fukunaga, and H. Nakae, *J. Cryst. Growth*, Vol 222, 2001, p 806–815

## SELECTED REFERENCE

- D.M. Stefanescu and R. Ruxanda, Fundamentals of Solidification, *Metallography and Microstructures*, Vol 9, *ASM Handbook*, ASM International, 2004, p 71–92